Annihilation probability density in positron scattering by He

Márcio T. do N. Varella, Claudia R. C. de Carvalho, and Marco A. P. Lima
Instituto de Física Gleb Wataghin, Universidade Estadual de Campinas, Unicamp, 13083-970 Campinas, São Paulo, Brazil

Euclimar P. da Silva
Departamento de Física, Universidade Federal do Ceará, 60455-760 Fortaleza, Ceará, Brazil

(Received 30 June 2000; published 13 April 2001)

We have calculated annihilation probability densities in positron collisions against the He atom. Our scattering wave functions were obtained with the Schwinger multichannel method [J. S. E. Germano and M. A. P. Lima, Phys. Rev. A **47**, 3976 (1993)]. It has been found that direct annihilation, in which electronic cloud deformation shields the nuclear repulsive potential effectively attracting the positron to a binary encounter, dominates the annihilation process at low impact energies. Closer to the real positronium formation threshold, the signature of virtual positronium has been noticed. At room temperature, significant annihilation probability has been observed over a somewhat extended region.

DOI: 10.1103/PhysRevA.63.052705 PACS number(s): 34.85.+x, 78.70.Bj

I. INTRODUCTION

In recent years, many theoretical and experimental papers have focused on annihilation on positron scattering by atoms and molecules. It has been found for molecular gases that measured annihilation rates are usually much larger than expected when e^+-target correlation effects are neglected [1] (i.e., proportional to Z, the number of target electrons). So far, the dynamical processes responsible for very high annihilation rates in molecular gases have remained controversial. A few different pathways have been proposed, based on the formation of virtual states [2,3], the formation of virtual positronium followed by pick-off annihilation (i.e., with one of the *other* molecular electrons) [4], nonresonant vibrational coupling [5], and vibrational Feshbach resonances [6].

While it is true that calculated and measured $Z_{\rm eff}$ values have clarified the understanding of the annihilation dynamics, we believe that such a powerful tool has not yet been fully explored. The reported theoretical papers have been limited to the integrated $Z_{\rm eff}$ value, given by

$$Z_{\rm eff}(k_i)=\frac{1}{4\pi}\int d\hat{k}_i\left\langle \Psi_{k_i}^{(+)}\left|\left[\sum_{j=1}^{Z}\delta(\vec{r}_j-\vec{r}_p)\right]\right|\Psi_{k_i}^{(+)}\right\rangle, \tag{1}$$

where $\Psi_{k_i}^{(+)}$ is the elastic scattering wave function. The definition above can be integrated over all electron coordinates, and the resulting integrand will be a function only of positron coordinates,

$$Z_{\rm eff}=\int d^3r\,\zeta_{\rm eff}(\vec{r}). \tag{2}$$

After appropriate normalization of $\zeta_{\rm eff}$ (the integrand of $Z_{\rm eff}$), one may assert that the probability of annihilation taking place between $\vec{r}$ and $\vec{r}+d\vec{r}$ will be given by

$$dP(\vec{r})=\frac{1}{Z_{\rm eff}}\zeta_{\rm eff}(\vec{r})d^3r\equiv\overline{\zeta}_{\rm eff}(\vec{r})d^3r. \tag{3}$$

Hence, the normalized integrand $\overline{\zeta}_{\rm eff}$ provides a spatial *annihilation probability density* (APD) in positron scattering, and annihilation maps can be readily obtained. It is worth mentioning that normalization of the integrand of $Z_{\rm eff}$ is always possible in low-energy collisions, i.e., below the real positronium formation threshold, even though the elastic scattering amplitude is not square-integrable. In the $Z_{\rm eff}$ definition, Eq. (1), the position operator assures that the integrand will be nonzero only in the interaction region, where positron and electron densities overlap.

To our knowledge, the integrand of $Z_{\rm eff}$ has only been studied by Van Reeth and Humberston [7]. These authors addressed the behavior of the annihilation parameter in the vicinity of the real positronium formation threshold, and calculated the integrand of $Z_{\rm eff}$ for e^+-H scattering in such a context. We believe the integrand of $Z_{\rm eff}$, as well as APD, to be much more useful in understanding the annihilation process in a broader sense. In this article we aim to illustrate, through a simple application, that APD may be of great help in the study of annihilation dynamics, perhaps bringing to light new information to the so far open discussion about the mechanisms underlying the high annihilation rates observed for molecules.

II. THEORY

Our elastic scattering wave functions were obtained with the Schwinger multichannel method (SMC) for positrons, which is extensively discussed elsewhere [8,9]. The SMC provides a variational expression for the scattering amplitude, from which the scattering wave function may be obtained,

$$|\Psi_{k_i}^{+}\rangle=\sum_{m,n}|\chi_m\rangle(A^{(+)-1})_{mn}\langle\chi_n|V|S_{k_i}^{+}\rangle, \tag{4}$$

where

$$A^{(+)}=Q\hat{H}Q+PVP-VG_P^{(+)}V. \tag{5}$$

In the above expressions, $S_{\vec{k}_i}$ is a solution of the unperturbed Hamiltonian (molecular Hamiltonian plus the kinetic-energy operator for the incident positron); V is the interaction potential between the incident positron and the molecular target; and $|\chi_m\rangle$ is a *configuration* state, i.e., an $(N+1)$-particle variational trial function (the product of a target state and a positron scattering orbital). P and Q are, respectively, projection operators onto energetically open and closed electronic states of the target; $\hat{H}$ is the collision energy minus the full scattering Hamiltonian; and $G_P^{(+)}$ is the free-particle Green's function projected on P space.

In the present calculations, only elastic scattering is considered and one therefore finds $P=|\Phi_0\rangle\langle\Phi_0|$, where $|\Phi_0\rangle$ is the target's ground state. Positron-target interaction may be treated in two levels of approximation, namely static (S) and static plus polarization (SP). In the former, the target is kept frozen in its ground state, and the configurations used to expand the trial scattering wave function take the form

$$|\chi_m\rangle=|\Phi_0\rangle\otimes|\varphi_m\rangle, \tag{6}$$

where φ_m is a positron scattering orbital. The SP approximation, on the other hand, takes polarization effects into account through single excitations of the $(N+1)$-particle compound system. The configurations are then given by

$$|\chi_{ij}\rangle=|\Phi_i\rangle\otimes|\varphi_j\rangle, \tag{7}$$

where Φ_i is a singly excited target state.

It should also be noted that the SMC method includes the asymptotic scattering boundary condition through the Green's function [9,10], allowing one to use Cartesian Gaussian basis sets to expand the scattering wave function. Even though Gaussian basis sets do not present appropriate asymptotic behavior, one is able to obtain reliable Z_{eff} values below the real positronium formation threshold, since the scattering wave function only needs to be accurately described in the interaction region, because of the position operator in Eq. (1).

Here we use target and scattering basis sets described by da Silva *et al.* [9], augmented with one *d* Cartesian Gaussian function centered on the nucleus (exponent 0.02). The target was treated as belonging to the D_{2h} point-symmetry group, because our computational codes were designed to deal with polyatomic targets. Partial contributions to the integrated Z_{eff} values are given in Table I at selected energies. All calculations took polarization effects into account (SP approximation), unless otherwise stated, and were performed below the real positronium threshold (18.17 eV in our model).

TABLE I. Symmetry decomposition of integrated Z_{eff} values.

Energy (eV)	Symmetry	Z_{eff}
0.0257	A_g	4.26
	$B_{1u}+B_{2u}+B_{3u}$	$\sim 10^{-3}$
	$B_{1g}+B_{2g}+B_{3g}$	$\sim 10^{-6}$
	A_u	$\sim 10^{-10}$
1.0	A_g	3.60
	$B_{1u}+B_{2u}+B_{3u}$	0.22
	$B_{1g}+B_{2g}+B_{3g}$	$\sim 10^{-3}$
	A_u	$\sim 10^{-6}$
5.0	A_g	2.81
	$B_{1u}+B_{2u}+B_{3u}$	0.88
	$B_{1g}+B_{2g}+B_{3g}$	$\sim 10^{-2}$
	A_u	$\sim 10^{-4}$
10.0	A_g	0.91
	$B_{1u}+B_{2u}+B_{3u}$	1.35
	$B_{1g}+B_{2g}+B_{3g}$	0.15
	A_u	$\sim 10^{-3}$
15.0	A_g	1.07
	$B_{1u}+B_{2u}+B_{3u}$	1.63
	$B_{1g}+B_{2g}+B_{3g}$	0.27
	A_u	$\sim 10^{-2}$

III. RESULTS AND DISCUSSION

Figure 1 shows the APD (normalized annihilation maps) for e^+-He collisions at 0.0257 (room temperature), 1, 5, 10, and 15 eV. The electronic density of the 1*s* atomic orbital (ρ_{1s}) is also presented. The APDs have been already integrated over all directions and only the radial dependence is shown. Below 5 eV, it is found that APD shapes are quite similar to that of ρ_{1s}, though shifted to the right because of nuclear repulsion. At 10 and 15 eV, however, that resemblance is no longer observed, and nonzero annihilation probability is found for $r>4a_0$. It should be observed that the integrand of Z_{eff} calculations for the H atom [7] did not show such a qualitative change as impact energies were increased. The more complex behavior observed for He may be related to many-body effects not present in e^+-H collisions, such as pick-off annihilation and screening of the nuclear repulsive potential by the *other* electron (the one that does not annihilate).

In Fig. 2 we show the APD and integrand of Z_{eff} at room

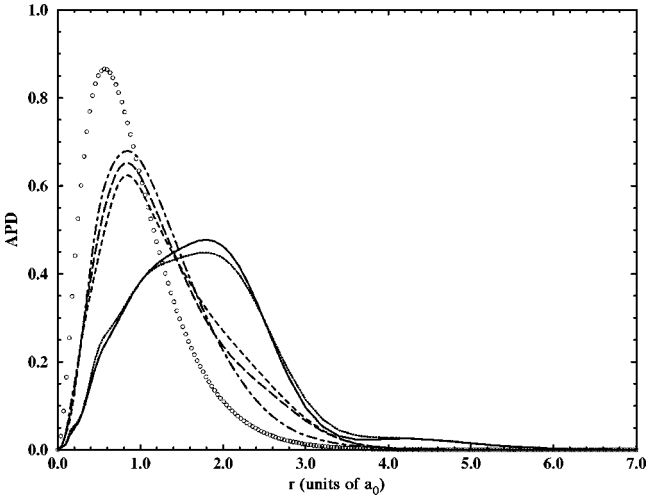

FIG. 1. Annihilation probability density (APD) for e^+-He scattering. Dot-dashed line, 0.0257 eV; long-dashed line, 1 eV; dashed line, 5 eV; dotted line, 10 eV; solid line, 15 eV; circles, ρ_{1s} (electronic density of the atomic 1*s* orbital).

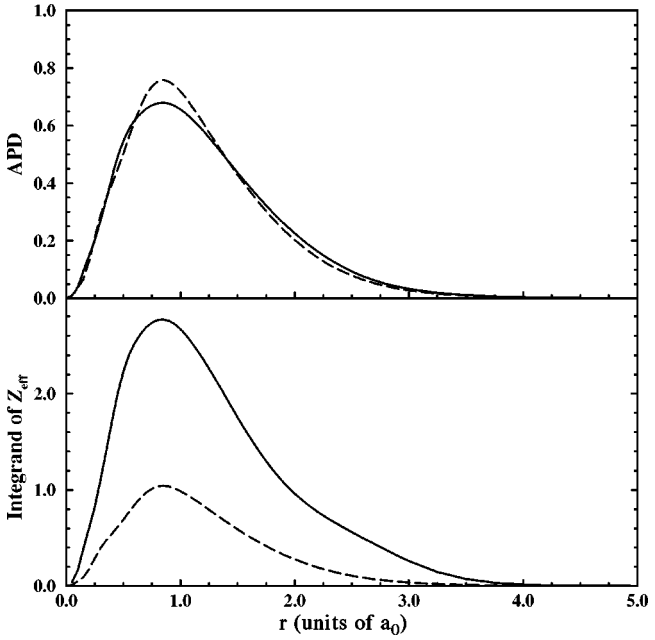

FIG. 2. Annihilation probability density (APD) and integrand of $Z_{\rm eff}$ at 0.0257 eV for e^+-He scattering. Solid line, SP approximation; dashed line, S approximation.

temperature obtained through static (S) and static-plus-polarization (SP) approximations. The fact that significant annihilation probabilities are observed over a somewhat extensive region (below $r \simeq 3a_0$) is very interesting. In principle, one could expect the effective annihilation region to be much narrower because electron density would drop quickly outside the atom and positron density would decrease rapidly inside it, due to the repulsive potential experienced by the projectile. Our results, however, indicate that annihilation may take place close to the nucleus even when deformation of the electronic cloud is neglected.

It should also be noted that polarization effects increase nearly four times the room-temperature $Z_{\rm eff}$ value of He (see the lower part of Fig. 2 and also da Silva *et al.* [9]), while APD extension is essentially the same in both S and SP calculations (see the upper part of Fig. 2). Hence, polarization effects enhance annihilation all over the target electronic cloud, especially in the range $2.5a_0 < r < 3.5a_0$ where the static integrand of $Z_{\rm eff}$ is negligible, even though annihilation is always restricted to the region $r < 4a_0$. One may therefore conclude that target relaxation shields the repulsive potential, attracting the positron to the nuclear vicinity. Hence, present APD calculations do not provide support to a recently proposed model [6] in which an expression for the fixed-nuclei contribution to the integrated $Z_{\rm eff}$ value is derived. In such a model, it is assumed that annihilation would take place over a very narrow shell, of radius R_a and width δR_a, and also that electron-positron interaction would be very weak in the valence region. (For the He atom, the shell radius was estimated to be $R_a = 3.9a_0$ [6], where essentially zero annihilation probability is found.)

Another interesting feature revealed by Fig. 1 is the nonzero annihilation probability beyond $r = 3.5a_0$ at 10 and 15 eV. Such ''tails'' in the APD are exclusively due to the A_g symmetry contribution, as discussed below. In Figs. 3 and 4 we show the APD for the A_g and B_{1u} global irreducible representations (IRs). The former essentially corresponds to the $l=0$ contribution, while the latter, to one of the three degenerate components ($m=0$) of the $l=1$ contribution. The tail in the APD is remarkable for the A_g component (Fig. 3), while it is not noticed for the B_{1u} component (Fig. 4). It should be observed that the APD for the B_{1u} IR is presented in two ways: (i) radial dependence (integrated over all directions) and (ii) axial dependence (integrated over the polar angle and cylindrical radius). The latter resembles the electron density of a p_z atomic orbital at all addressed energies, unlike the A_g APD, which is similar to ρ_{1s} electron density only at low impact energies (see Fig. 1). Though not shown here, B_{xg} ($x=1,2,3$) and A_u symmetries do not present remarkably different APD shapes as incident energy is raised. (They also provide very modest contributions to the overall

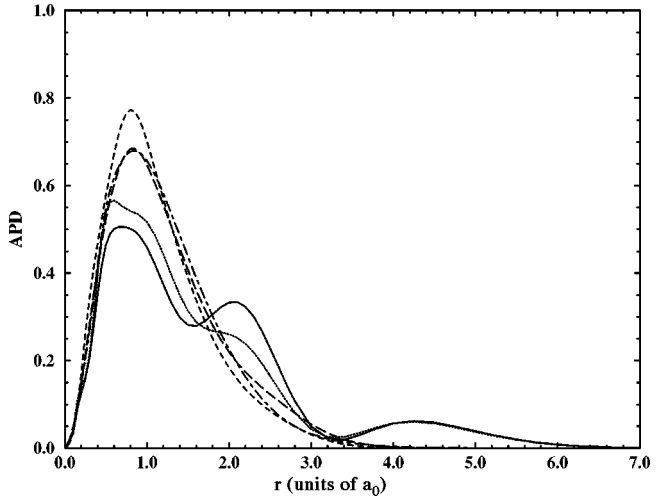

FIG. 3. A_g component of the APD for e^+-He scattering. Dot-dashed line, 0.0257 eV; long-dashed line, 1 eV; dashed line, 5 eV; dotted line, 10 eV; solid line, 15 eV.

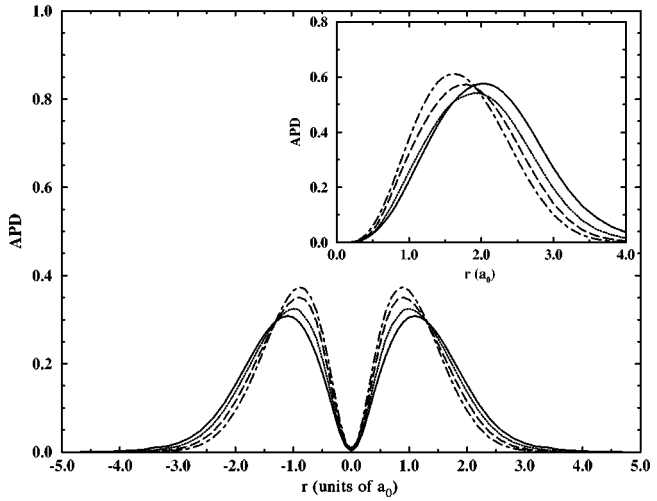

FIG. 4. B_{1u} component of the APD for e^+-He scattering. Both axial and radial (offset) dependences are shown. Solid line, 1.0 eV; dotted line, 5 eV; dashed line, 10 eV; dot-dashed line, 15 eV.

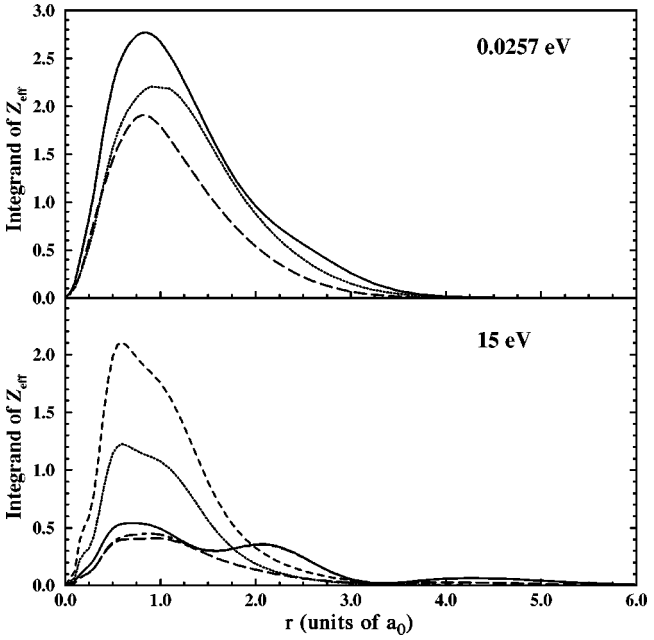

FIG. 5. Integrand of Z_{eff} for the He atom. Top, 0.0257 eV. Solid line, result obtained with all $(N+1)$-particle configurations; dashed line, result obtained only with configurations associated with target states with energies above 30 eV; dotted line, result obtained only with configurations associated with target states with energies below 60 eV. Bottom, 15 eV. Results obtained only including configurations associated with target states with energies up to 30 eV (dotted line), 50 eV (dashed line), 60 eV (long-dashed line), 70 eV (dot-dashed line), all configurations (solid line).

Z_{eff} values, due to higher angular-momentum barriers. See Table I.)

The bump observed in the A_g component of the APD around $r=4.5a_0$ (10 and 15 eV) may correspond to a signature of virtual positronium formation. The fact that it only shows up in the A_g component should be expected, due to the following argument. If a positronium atom approaches an $(N-1)$-electron target at a very low incident energy ($E \simeq 0$), the rearrangement reaction would lead to a neutral N-electron target plus a positron with energy just above the real positronium formation of the inverse process. In such a case, scattering would be described by the s wave, due the absence of an angular-momentum barrier, i.e., by the totally symmetric IR contribution. Considering the inverse process, in which a positron with energy slightly above the real positronium formation threshold collides against a neutral target, one should also observe positronium formation in the totally symmetric IR.

To gain further insight into the virtual positronium formation signature in the APD, we show in Fig. 5 the integrand of Z_{eff} (nonnormalized annihilation maps) for the A_g symmetry at 0.0257 and 15 eV. At room temperature, we show three different calculations: (i) including all $(N+1)$-particle configurations; (ii) only including configurations associated with target states with energies above 30 eV; and (iii) only including configurations associated with target states with energies below 60 eV. The calculated electronic spectrum of the He atom (eigenvalues of the target Hamiltonian in closed-channel space) below 90 eV is presented in Fig. 6. At 0.0257 eV, it is clear that the 15 low-lying states below 30 eV (counting degeneracies) are more important to the overall Z_{eff} value than the 48 higher ones (above 60 eV). This behavior could be predicted by first-order perturbation theory and suggests that only ordinary polarization effects are taking place, as previously proposed for the N_2 molecule [3]. (Both N_2 and He, unlike C_2H_2, never showed any evidence of virtual state formation.) At 15 eV, we present results obtained with the inclusion of configurations associated with states with energies up to 30, 50, 60, and 70 eV, as well as with the whole configuration space. This time a dramatically different picture is found. It is clear that target states up to 50 eV are not at all able to describe the annihilation tail, being very far from convergence. States with energies between 50 and 60 eV cause a qualitative change, sketching the annihilation tail, but excitations above 60 eV are crucial to attain full convergence at larger radii. Hence, the bump in the APD (annihilation ''tail'') is clearly associated with highly excited target states. Since a suitable description of a virtual positronium in the periphery of the target must require configurations associated with excited target states, we understand that such a bump at larger radii—only observed in the A_g symmetry and associated with highly excited target states—is indeed a signature of virtual positronium formation.

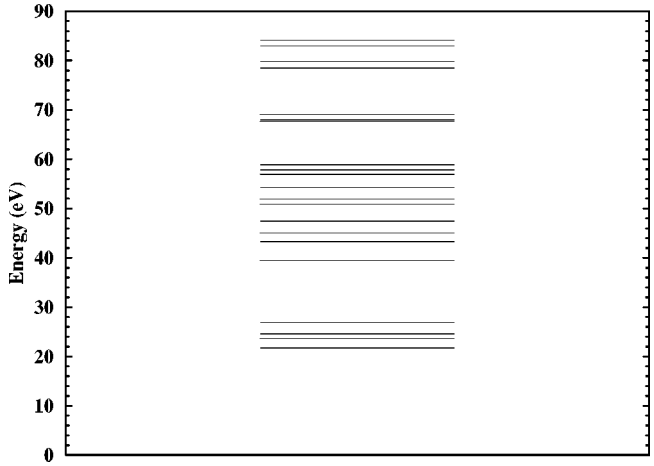

FIG. 6. Calculated electronic spectrum of the He atom.

IV. CONCLUSIONS

Through the calculation of annihilation maps, it was observed that direct annihilation, in which ordinary polarization effects effectively attract the positron to a binary encounter with an electron, prevails at low impact energies. Closer to the positronium formation threshold, the signature of virtual positronium was noticed. Our results suggest that annihilation takes place all over the target's 1s electronic density in room-temperature collisions, and not in a very thin shell at the outer valence region, as one might expect.

ACKNOWLEDGMENTS

This work was supported by the Brazilian agencies CNPq, CAPES, and FAPESP. Our calculations were partially performed at CENAPAD-SP.

[1] K. Iwata, R.G. Greaves, T.J. Murphy, M.D. Tinkle, and C.M. Surko, Phys. Rev. A **51**, 473 (1995).
[2] D.A.L. Paul and L. Saint-Pierre, Phys. Rev. Lett. **11**, 493 (1963); V.I. Goldanskii and YU.S. Sayasov, Phys. Lett. **13A**, 300 (1964).
[3] C. R. C. de Carvalho, M. T. do N. Varella, E. P. da Silva, J. S. E. Germano, and M. A. P Lima (unpublished).
[4] G. Laricchia and C. Wilkin, Phys. Rev. Lett. **79**, 2241 (1997).
[5] F.A. Gianturco, Europhys. Lett. **48**, 519 (1999).
[6] G.F. Gribakin, Phys. Rev. A **61**, 022720 (2000); K. Iwata, G.F. Gribakin, R.G. Greaves, C. Kurz, and C.M. Surko, *ibid.* **61**, 022719 (2000).
[7] P. Van Reeth and J.W. Humberston, J. Phys. B **31**, L231 (1998).
[8] J.S.E. Germano and M.A.P. Lima, Phys. Rev. A **47**, 3976 (1993).
[9] E.P. da Silva, J.S.E. Germano, and M.A.P. Lima, Phys. Rev. A **49**, R1527 (1994).
[10] E.P. da Silva, J.S.E. Germano, and M.A.P. Lima, Phys. Rev. Lett. **77**, 1028 (1996).